Demonstration of Widely Tunable Single-Chip 10-Gb/s Laser–Modulators Using Multiple-Bandgap InGaAsP Quantum-Well Intermixing

James W. Raring, *Student Member, IEEE*, Erik J. Skogen, *Member, IEEE*, Leif A. Johansson, Matt N. Sysak, Jonathon S. Barton, *Student Member, IEEE*, Milan L. Mašanoviæ, *Student Member, IEEE*, and Larry A. Coldren, *Fellow, IEEE*

***Abstract*—High-speed wavelength-agile laser–modulators were fabricated for the first time using a quantum-well intermixing processing platform for monolithic integration. Over 19-GHz 3-dB modulator bandwidth was achieved and 10-Gb/s error-free transmission was demonstrated through 75 km of standard fiber.**

***Index Terms*—Electroabsorption modulators (EAMs), ion implantation, laser tuning, quantum-well intermixing (QWI), semiconductor lasers, wavelength-division multiplexing.**

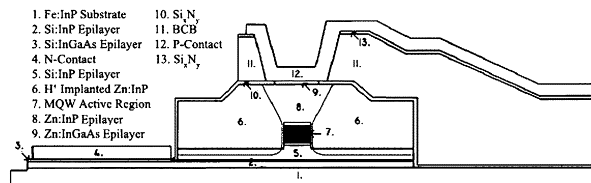

Fig. 1. Cross-sectional schematic of modulator sections, illustrating the placement of BCB and the angled implant profile used for capacitance reduction.

I. Introduction

PHOTONIC integrated circuits (PICs) with wavelength-agile capabilities are key to next-generation optical networks employing wavelength-division multiplexing. Widely tunable transmitters will provide cost savings through inventory reduction and will facilitate the enabling technologies for future applications such as dynamic provisioning and wavelength routing.

The work presented here utilizes quantum-well intermixing (QWI) to provide device-specific band-edge definition orthogonal to the growth direction [1] for the realization of high performance wavelength-agile transmitters at 10 Gb/s. We demonstrate, for the first time, 10-Gb/s operation across the tuning band of a widely tunable laser using partially quantum-well-intermixed material in an integrated electroabsorption modulator (EAM). The viability of the devices for high-speed transmission applications was confirmed with the first demonstration of 10-Gb/s transmission using a widely tunable sampled-grating (SG) distributed Bragg reflector (DBR) laser/EAM transmitter. The device exhibited error-free/low-dispersion-penalty transmission through 75 km of standard fiber and a small signal chirp parameter capable of being tuned to negative values.

II. Experiment

The transmitter device consists of a five-section widely tunable SG-DBR laser followed by an EAM. The five sections of the SG-DBR laser are, from rear facet to front facet, backside absorber, rear mirror, phase, gain, and front mirror. The phase and mirror sections function to tune the wavelength of the laser [2]. The lithographically defined mirrors make the SG-DBR laser ideal for monolithic integration due to the fact that no facets are required for operation.

This work employs a modified ion-implantation enhanced QWI process described in [1], as the fabrication platform. In this process, an InP buffer layer, situated above the multiquantum-well (MQW) active region, functions to capture the vacancies created during an ion implantation. During a high-temperature anneal, the vacancies are diffused through the MQW region, promoting the interdiffusion of group V-atoms between the wells and barriers. The interdiffusion reshapes the quantum-well profile by distorting the quantum-well–barrier interface. The result is a shift in the quantized energy levels in the well, and hence, a shift in the band edge energy [3].

Several design and processing measures were taken to reduce parasitic capacitance in the EAM regions to achieve 10-Gb/s operation. The epilayer base structure was grown on a semi-insulating substrate. A 3-μm-thick layer of benzocyclobutene (BCB) was defined below the EAM bond pads to serve as a low-K dielectric. An angled proton implantation was performed adjacent to the buried ridge to eliminate the parasitic capacitance associated with the homojunction. The implant was designed such that proton concentration was maintained at a level greater than 2E19 cm^{-2} to a depth beyond the InP homojunction on either side of the buried ridge. Fig. 1 is a schematic cross-sectional view of the EAM, illustrating these described features.

III. Fabrication

The metal–organic chemical vapor deposition (MOCVD)-grown epitaxial base structure contained an n-contact InGaAs layer 1 μm below an MQW active region centered within a

Manuscript received February 4, 2004; revised March 30, 2004. This work was supported by Defense Advanced Research Projects Agency (DARPA)/MTO CS-WDM under Grant N66001-02-C-8026 and by Intel Corporation under Grant TXA001 630 000.

The authors are with the Materials Engineering Department, University of California, Santa Barbara, CA 93106 USA (e-mail: jraring@engineering.ucsb.edu).

Digital Object Identifier 10.1109/LPT.2004.828853

1041-1135/04$20.00 © 2004 IEEE

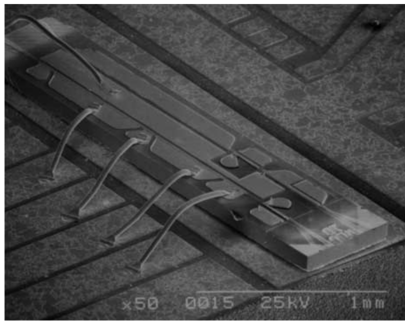

Fig. 2. Electron micrograph of transmitter device.

1.1Q waveguide. The MQW consists of 15 InGaAsP 8.0-nm compressively strained (0.6%) quantum wells, separated by 8.0-nm tensile-strained (0.3%) InGaAsP barriers grown on a Fe-doped InP substrate. Following the active region, a 15-nm InP stop etch, a 20-nm 1.3Q stop etch, and a 450-nm InP implant buffer layer was grown.

The process was as follows: The gain sections and the absorber sections were masked with 500 nm of Si_xN_y and the sample was subjected to a P^+ implant at 100 keV and a dose of 5E14 cm^{-2}, yielding a range of 900 Å into the implant buffer layer. The sample was subjected to rapid thermal processing at a temperature of 675 °C, promoting the diffusion of vacancies through the MQW region. Once the desired band-edge for the EAM was achieved ($\lambda_{pl} = 1510$ nm) the diffusion process was halted. The implant buffer layer above the EAM sections was removed using a wet etch process, stopping on the 1.3Q stop etch layer. The sample was then subjected to an additional rapid thermal anneal, further blue-shifting the regions where the implant buffer layer remained. This second anneal was used to obtain desired band edge ($\lambda_{pl} = 1450$ nm) for the mirror, phase, and passive waveguide sections.

The remainder of the process was carried out as described in [1] with the modifications for top-side n-contacts and the addition of BCB beneath the EAM contacts. The wafers were thinned and the devices were cleaved into bars and antireflection coated. The die were separated, soldered to aluminum nitride carriers, and wire bonded (Fig. 2) for characterization.

IV. RESULTS

The SG-DBR lasers demonstrated low threshold currents of 13 mA, with an output power of 10 mW at a gain section current of 100 mA. At this operating point, a sidemode suppression ratio (SMSR) greater than 35 dB was achieved. The devices demonstrated over 25 nm of wavelength tunability. For the testing discussed in this letter, the rear mirror was held at a bias of 0 mA while the front mirror was biased at levels between 0 and 15 mA to tune across super modes within the tuning range. The low threshold current can be attributed to the high modal gain offered by the centered quantum-well design. This design results in optimum modal overlap with the quantum wells, increasing the confinement factor by 50% over the offset quantum-well architecture found in traditional SG-DBR laser designs [4]. The dc modal extinction characteristics of a 175-μm-long EAM are presented in Fig. 3. Over 40 dB of extinction was demonstrated for wavelengths of 1558, 1570, and 1580 nm, with efficiencies greater than 20 dB/V. The efficient extinction properties are due

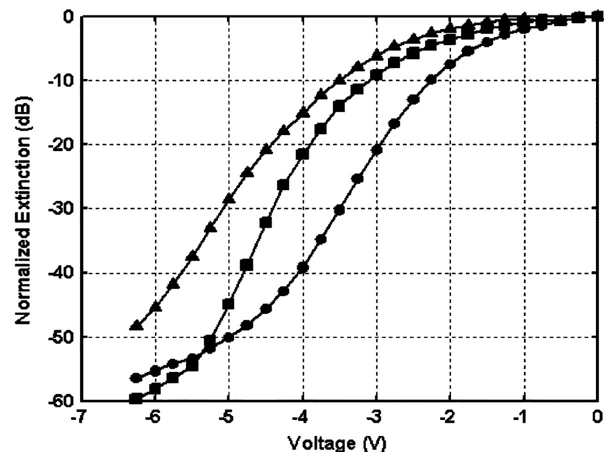

Fig. 3. DC extinction of a 175-μm modulator for wavelengths of 1558 (circles), 1570 (squares), and 1580 nm (triangles).

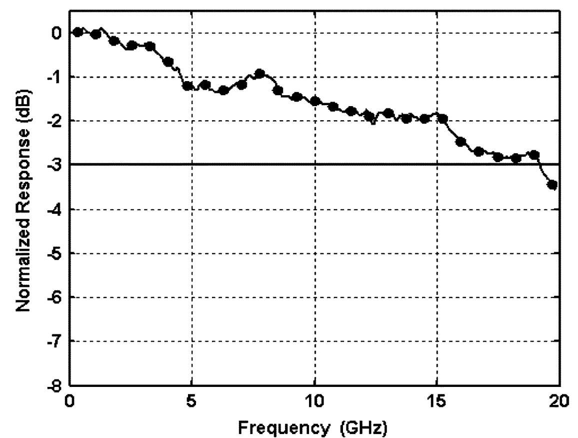

Fig. 4. Electrical to optical frequency response of a 175-μm modulator. The circular markers represent every 30th data point.

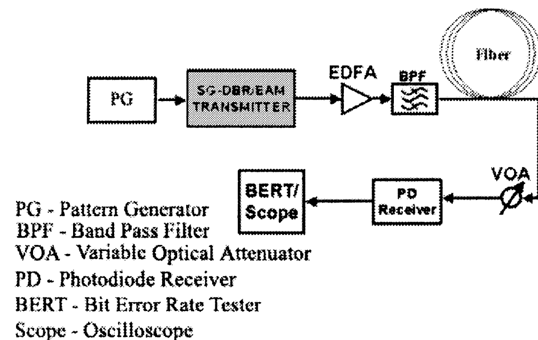

Fig. 5. Test set used to obtain BER and eye-diagrams from transmitter.

to the combination of the centered quantum-well design and the intermixing process that allows for precise placement of the modulator band edge. The 3-dB bandwidth of the same modulator was greater than 19 GHz, as shown in Fig. 4.

To demonstrate operation and transmission at 10 Gb/s, eye diagrams were taken and bit-error-rate (BER) testing was performed through various fiber lengths for the SG-DBR/EAM transmitters. BER testing was performed using a pseudorandom bit sequence of $2^{31}-1$. A schematic of the test setup is shown in Fig. 5. Eye diagrams, shown in Fig. 6, were taken at wavelengths of 1558, 1564, 1571, and 1578 nm with dc biases ranging from

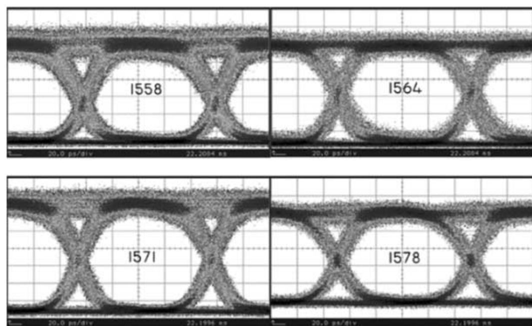

Fig. 6. Back-to-back eye diagrams from transmitter at wavelengths of 1558, 1564, 1571, and 1578 nm.

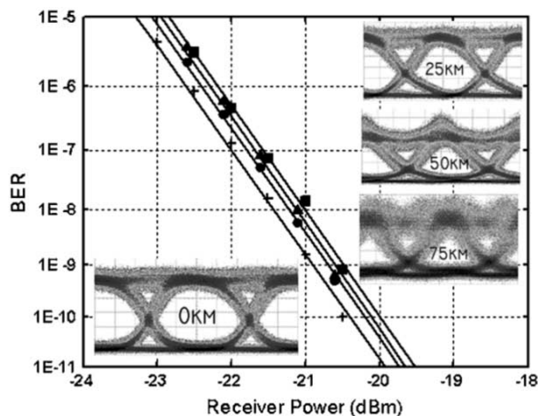

Fig. 7. BER curves and respective eye diagrams for back-to-back (cross), and transmission through 25 (circles), 50 (triangles), and 75 km (squares) of fiber at a wavelength of 1564 nm.

−2.1 to −3.8 V and peak-to-peak voltage swings ranging from 2.2 to 3.4 V. Greater than 10-dB extinction was achieved at all wavelengths. We believe that the less efficient dynamic extinction behavior compared to the dc behavior is due to the use of an erbium-doped fiber amplifier (EDFA) and the application of a lower gain section bias (50 mA) during dynamic testing. The amplified spontaneous emission from the EDFA significantly raises the noise floor, decreasing the amount of total extinction read by the digital communications analyzer. The higher gain section bias (100 mA) used during dc testing will result in a greater amount of optical power entering the EAM, creating more heat, inducing more bandgap shrinkage, and hence increasing the absorption efficiency. Fig. 7 presents BER results and eye-diagrams for back-to-back and through 25, 50, and 75 km of Corning SMF-28 fiber at a wavelength of 1564 nm and a dc bias of −3.4 V. Error-free operation was achieved through 75 km of fiber, with a dispersion power penalty of less than 0.5 dB. The variation in the signal-to-noise ratio in the eyes of Fig. 7 is due to receiver noise, which becomes more pronounced as the received optical power decreases with longer fiber spans.

The low dispersion penalties of Fig. 7 are indicative of a slightly negative large signal chirp parameter. Using the fiber response frequency domain method described in [5], the small signal chirp parameter of the device was extracted for various EAM bias points at 1564 nm, as shown in the inset of Fig. 8. The transition from a positive to a negative chirp parameter occurred at −3.5 V. To demonstrate the capability for efficient 10-Gb/s

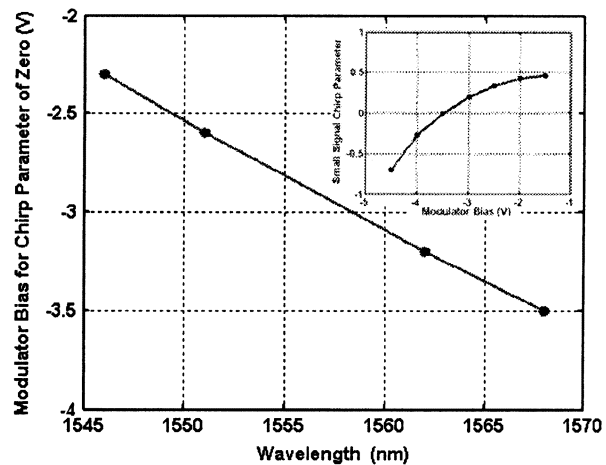

Fig. 8. Required EAM bias to achieve small signal chirp parameter of zero versus operating wavelength. The inset depicts the small signal chirp parameter characteristics versus reverse bias at 1563 nm for a separate device.

transmission across the wide tuning range of the devices, small signal chirp parameters were extracted at wavelengths of 1546, 1552, 1563, and 1568 nm on a separate device. At all wavelengths tested, the chirp parameter was shown to go negative, requiring a larger reverse bias with increasing wavelength. The required EAM bias points to achieve a chirp parameter of zero at these wavelengths are shown in Fig. 8. This behavior is expected since a larger reverse bias is required at longer wavelengths to position the EAM band edge at the correct proximity to the operating wavelength.

V. Conclusion

A QWI processing platform coupled with several measures for capacitance reduction were utilized for the realization of high-performance widely tunable transmitters. The 175-μm EAMs possessed a dc absorption efficiency of over 20 dB/V, radio-frequency extinctions greater that 10 dB, and over 19-GHz 3-dB bandwidth. Error-free transmission through 75 km of fiber was demonstrated with a monolithically integrated laser–modulator operating at 10 Gb/s. The power penalty of transmission was less than 0.5 dB, indicative of a negative large signal chirp parameter. The small signal chirp parameter was extracted and was shown to go negative across the tuning range of the device.

References

[1] E. Skogen, J. Raring, J. Barton, S. DenBaars, and L. Coldren, "Post-growth control of the quantum-well band edge for the monolithic integration of widely-tunable lasers and electroabsorption modulators," *J. Select. Topics Quantum Electron.*, vol. 9, pp. 1183–1190, Sept./Oct. 2003.

[2] V. Jayaraman, Z. Chuang, and L. Coldren, "Theory, design, and performance of extended tuning range semiconductor lasers with sampled gratings," *IEEE J. Quantum Electron.*, vol. 29, pp. 1824–1834, June 1993.

[3] E. Skogen, J. Barton, S. DenBaars, and L. Coldren, "Tunable sampled-grating DBR lasers using quantum-well-intermixing," *IEEE Photon. Technol. Lett.*, vol. 14, pp. 1243–1245, Sept. 2002.

[4] B. Mason, J. Barton, G. Fish, and L. Coldren, "Design of sampled grating DBR lasers with integrated semiconductor optical amplifiers," *IEEE Photon. Technol. Lett.*, vol. 12, pp. 762–764, July 2000.

[5] B. Dvaux, Y. Sorel, and J. F. Kerdiles, "Simple measurement of fiber dispersion and of chirp parameter of intensity modulated light emitter," *J. Lightwave Technol.*, vol. 11, pp. 1937–1940, Dec. 1993.